ARTICLE OPEN ACCESS

GRP78 Antibodies Are Associated With Blood-Brain Barrier Breakdown in Anti–Myelin Oligodendrocyte Glycoprotein Antibody–Associated Disorder

Fumitaka Shimizu, MD, PhD, Ryo Ogawa, MD, PhD, Yoichi Mizukami, MD, PhD, Kenji Watanabe, PhD, Kanako Hara, Chihiro Kadono, Toshiyuki Takahashi, MD, PhD, Tatsuro Misu, MD, PhD, Yukio Takeshita, MD, PhD, Yasuteru Sano, MD, PhD, Miwako Fujisawa, MD, Toshihiko Maeda, MD, PhD, Ichiro Nakashima, MD, PhD, Kazuo Fujihara, MD, PhD, and Takashi Kanda, MD, PhD

Correspondence
Dr. Kanda
tkanda@yamaguchi-u.ac.jp

Neurol Neuroimmunol Neuroinflamm 2022;9:e1038. doi:10.1212/NXI.0000000000001038

Abstract

Background and Objectives

To analyze (1) the effect of immunoglobulin G (IgG) from patients with anti–myelin oligodendrocyte glycoprotein antibody (MOG-Ab)–associated disorder on the blood-brain barrier (BBB) endothelial cells and (2) the positivity of glucose-regulated protein 78 (GRP78) antibodies in MOG-Ab–associated disorders.

Methods

IgG was purified from sera with patients with MOG-Ab–associated disorder in the acute phase (acute MOG, n = 15), in the stable stage (stable MOG, n = 14), healthy controls (HCs, n = 9), and disease controls (DCs, n = 27). Human brain microvascular endothelial cells (BMECs) were incubated with IgG, and the number of nuclear NF-κB p65-positive cells in BMECs using high-content imaging system and the quantitative messenger RNA change in gene expression over the whole transcriptome using RNA-seq were analyzed. GRP78 antibodies from patient IgGs were detected by Western blotting.

Results

IgG in the acute MOG group significantly induced the nuclear translocation of NF-κB and increased the vascular cell adhesion molecule 1/intercellular adhesion molecule 1 expression/permeability of 10-kDa dextran compared with that from the stable MOG and HC/DC groups. RNA-seq and pathway analysis revealed that NF-κB signaling and oxidative stress (NQO1) play key roles. The NQO1 and Nrf2 protein amounts were significantly decreased after exposure to IgG in the acute MOG group. The rate of GRP78 antibody positivity in the acute MOG group (10/15, 67% [95% confidence interval, 38%–88%]) was significantly higher than that in the stable MOG group (5/14, 36% [13%–65%]), multiple sclerosis group (4/29, 14% [4%–32%]), the DCs (3/27, 11% [2%–29%]), or HCs (0/9, 0%). Removal of GRP78 antibodies from MOG-IgG reduced the effect on NF-κB nuclear translocation and increased permeability.

Discussion

GRP78 antibodies may be associated with BBB dysfunction in MOG-Ab–associated disorder.

From the Department of Neurology and Clinical Neuroscience, Yamaguchi University Graduate School of Medicine (F.S., K.H., C.K., Y.T., Y.S., M.F., T. Maeda, T.K.), Ube; Department of Neurology, Tohoku University Graduate School of Medicine (R.O., T.T., T. Misu), Sendai; Center for Gene Research (Y.M., K.W.), Yamaguchi University (Y.M., K.W.), Ube; Department of Neurology, National Hospital Organization Yonezawa Hospital (T.T.); Department of Neurology, Tohoku Medical and Pharmaceutical University (I.N.), Sendai; and Department of Multiple Sclerosis Therapeutics, Fukushima Medical University (K.F.), Japan.

Go to Neurology.org/NN for full disclosures. Funding information is provided at the end of the article.

The Article Processing Charge was funded by the authors.

Glossary

ADEM = acute disseminated encephalomyelitis; **ANOVA** = analysis of variance; **BBB** = blood-brain barrier; **BMEC** = brain microvascular endothelial cell; **CBA** = cell-based assay; **CE** = cortical encephalitis; **CI** = confidence interval; **DC** = disease control; **EAE** = experimental autoimmune encephalomyelitis; **EDSS** = Expanded Disability Status Scale; **FC** = fold change; **GRP 78** = glucose-regulated protein 78; **HC** = healthy control; **ICAM-1** = intercellular adhesion molecule 1; **IgG** = immunoglobulin G; **IPA** = ingenuity pathway analysis; **MOG** = myelin oligodendrocyte glycoprotein; **MOG-Ab** = myelin oligodendrocyte glycoprotein antibody; **MS** = multiple sclerosis; **NMO** = neuromyelitis optica; **NMOSD** = neuromyelitis optica spectrum disorder; **ON** = optic neuritis; **PBS** = phosphate-buffered saline; **PVDF** = polyvinylidene difluoride; **VCAM-1** = vascular cell adhesion molecule 1.

Anti–myelin oligodendrocyte glycoprotein antibody (MOG-Ab)–associated disorder has been recently recognized as a new entity in the spectrum of inflammatory demyelinating diseases, differing from either multiple sclerosis (MS) or neuromyelitis optica spectrum disorder (NMOSD).[1-4] Using live cell-based assays (CBAs), MOG antibodies bound to the cell surface are detected in patients with pediatric/adult acute disseminated encephalomyelitis (ADEM), AQP4 antibody–negative NMOSD, isolated optic neuritis, transverse myelitis, encephalomyelitis, or brainstem encephalitis.[2] The clinical spectrum of MOG-Ab–associated disorder thus seems to be broader than that of AQP4 antibody–positive NMOSD,[3,4] but what factors determine the varied clinical phenotypes of the disease remain unclear.

A previous histopathologic analysis of 9 cases with MOG-Ab–associated disorder described an MS pattern II lesion, characterized by active demyelination with marked infiltration of macrophages and T cells, along with deposition of immunoglobulin G (IgG)/complements,[5-9] suggesting Ab-mediated demyelination. Intrathecal transfer experiments of MOG-Abs from patients with MOG-Ab–associated disorder to experimental autoimmune encephalomyelitis (EAE) models induced pathologic changes, resembling an MS pattern II pathology, together with myelin-reactive T cells (myelin basic protein–specific T cells) and MOG-specific T cells.[10] These findings suggest that MOG-Abs exert a pathogenic effect when they enter the CNS space in cases of MOG-Ab–associated disorder.

Blood-brain barrier (BBB) breakdown is a key pathologic feature of MS and neuromyelitis optica (NMO).[11-14] We previously reported the effect of glucose-regulated protein 78 (GRP 78) autoantibodies from patients with NMO on human brain microvascular endothelial cell (BMEC) dysfunction.[15,16] Both a history of preceding infectious prodrome in 50% of patients with MOG-Ab–associated disorder[17] and the absence of oligoclonal IgG bands in the CSF[18] suggest that anti-MOG antibodies are produced peripherally and reach the CNS following BBB breakdown, but the molecular mechanism regarding BBB disruption in MOG-Ab–associated disorder remains unclear.

In the present study, we analyzed the contribution of serum IgG from individual patients with MOG-Ab–associated disorder to BBB breakdown using human BMECs with the high-content imaging and RNA-seq. We also investigated the GRP78 antibody positivity of patients and the effect of this antibody on the BMEC activation in MOG-Ab–associated disorder.

Methods

Patient Samples

This research was approved by the ethics committees of the Medical Faculties of Yamaguchi Universities (IRB#: H22-137-6). We obtained written informed consent from each participant.

Sera were collected from 15 patients with MOG-Ab–associated disorder who had been diagnosed at Tohoku University or Yamaguchi University Hospital (Table). All the patients were positive for MOG-Abs according to a cell-based assay performed at Tohoku University. We included sera from MOG-Ab–associated disorder patients (15 sera in the acute phase [acute MOG, n = 15] and 14 sera in the stable stage [stable MOG, n = 14]) (Table). The 15 serum samples from acute MOG were collected during the acute phase within 14 days at the time of the symptom onset, and the 14 sera from stable MOG were collected in the clinical stable phase from patients, who had been treated with corticosteroids over 3 months (3–57 months) after the acute phase. IgGs from 9 healthy controls (HCs: men, n = 4, women, n = 5; mean age, 32.6 years) and 27 disease controls (DCs) were used as controls (amyotrophic lateral sclerosis, n = 17; cervical spondylosis, n = 2; multiple system atrophy, n = 3; spinocerebellar degeneration, n = 1; hereditary peripheral neuropathy, n = 2; progressive supranuclear palsy, n = 1; and normal pressure hydrocephalus, n = 1).

All sera were stored at −80°C until the experiments were performed. Sere were inactivated at 56°C for 30 minutes before the experiments. IgG was prepared from serum samples using a Melon Gel IgG Spin Purification Kit (Thermo Fisher Scientific).

Patient Information

We investigated the clinical phenotype, the age/sex, the relapse number, ΔEDSS score (change in the score on the Expanded Disability Status Scale [EDSS] between before and after relapse), presence of a preceding infection, IgG index (intrathecal IgG synthesis), Q Albumin (Q Alb, BBB

Table Clinical Information of MOG Patients

Pt Nos.	Clinical phenotype	Age/ sex	Relapse number	ΔEDSS score	Preceding infection	IgG index	Q Alb	Gd-MRI	MOG-Ab	GRP Ab	% NFκB	Permeability
1	ON + M	30/M	1	5	(−)	0.5	4.0	(−)	32768	(+)	9.36	0.65
2	CE	41/M	1	5	(+)	0.54	21.0	(−)	1024	(−)	2.62	0.32
3	ON + M	16/M	1	5	(−)	0.64	3.9	(−)	512	(+)	2.61	0.36
4	CE	36/M	1	5	(−)	0.56	5.9	(−)	16384	(+)	1.57	0.33
5	CE	39/M	1	2	(−)	NE	5.6	(−)	4096	(+)	6.47	0.43
6	CE	23/M	2	2	(−)	0.67	12.6	(−)	2048	(−)	0.35	0.37
7	CE	29/F	1	2	(−)	0.59	6.9	(−)	1024	(+)	0.11	0.38
8	ON + M	31/M	1	4	(−)	0.6	9.0	(+)	4096	(−)	0.55	0.40
9	ON + M	32/F	1	5	(+)	0.61	7.7	(−)	4096	(+)	11.8	0.56
10	ON	12/M	2	3.5	(+)	0.69	7.9	(−)	2048	(+)	0.19	0.31
11	ON + M	58/F	1	4	(−)	0.57	7.2	(−)	1024	(+)	0.41	0.36
12	ON	67/F	1	2	(−)	NE	NE	(−)	1024	(−)	3.94	0.40
13	ADEM	3/F	1	3.5	(−)	NE	NE	(−)	8192	(−)	0.71	0.32
14	ADEM	47/M	2	4.5	(−)	0.58	6.7	(+)	4096	(+)	0.30	0.34
15	ON	42/M	1	4	(−)	NE	NE	(−)	1024	(+)	0.33	0.33

Abbreviations: ADEM = acute disseminated encephalomyelitis; CE = cortical encephalitis; EDSS = Expanded Disability Status Scale; Gd-MRI = presence of Gd-enhanced spinal lesions on MRI; GRP Ab = presence of GRP78 autoantibodies in IgG from patients; M = myelitis; NE = not examined; ON = optic neuritis; preceding infection = presence of preceding infection; Pt Nos = patient numbers.
%NFκB, % of NF-κB p65 nuclear-positive cells; ΔEDSS score, change in the score on the EDSS from before to after relapse.

breakdown), and the presence of Gd-enhanced lesions on MRI in the 15 patients with acute MOG-Ab–associated disorder (Table).

Immunohistochemistry of NF-κB, ICAM-1, NOQ1, or Nrf2 and the High-Content Imaging Assay

TY10 cells derived from human adult BMECs and immortalized with temperature-sensitive SV40 large T antigen (tsA58) were used for experiments.[19] Two days after the shift in temperature from 33 to 37°C, all experiments were performed. The cells were maintained on collagen type 1–coated 96-well plates (Greiner) and then cultured in MCDB 131 medium containing IgG (500 μg/mL) from patients with MOG-Ab–associated disorder, DCs, or HCs after substitution for MCDB 131 medium for 1 hour for NF-κB p65 immunostaining and for 24 hours for intercellular adhesion molecule 1 (ICAM-1), NAD(P)H quinone dehydrogenase 1 (NQO1), Nrf2, and JC-1 immunostaining.

For NF-κB p65, NQO1, or Nrf2 staining, cells were fixed with 4% paraformaldehyde, incubated with 0.3% Triton X-100, and then blocked overnight in 5% fetal bovine serum/0.3% Triton X-100 in phosphate-buffered saline (PBS). The cells were incubated with each primary Abs (NF-κB p65 monoclonal antibody, NQO1 polyclonal antibody [Proteintech], or Nrf2 polyclonal antibody [Proteintech]), followed by the incubation with secondary Abs (Alexa Fluor 488 goat anti-rabbit IgG, Thermo Fisher Scientific).

For JC-1 staining, a final concentration of 1 μM of JC-1 MitoMP Detection Kit (DOJINDO, Japan) was added to living TY10 cells in the dark at 37°C for 45 minutes. JC-1 dye shows fluorescence emission at 2 typical wavelengths: red fluorescent J-aggregates at higher mitochondrial concentrations reflecting higher mitochondrial potential and green fluorescent J-monomers. The red/green intensity ratio reflects the mitochondria potential.

For high-content imaging,[16] 5,000 cells per well were plated onto CELLSTAR 96-well plates (Greiner). After immunostaining for NF-κB p65 was performed, the images in the plate were captured using an In Cell Analyzer 2000 (GE Healthcare) at ×20 magnification with 4 fields of view per well (equivalent to almost 800 cells). The images were then analyzed with the IN Carta image analysis software (Cytiva) or the In Cell Analyzer software program (Cytiva). The data represent the mean value of 12 experiments for NF-κB p65 or 3 experiments for ICAM-1, NQO1, Nrf2, and JC-1.

Paracellular Permeability of 10-kDa Dextran

TY10 cells were cultured on 0.4-mm pore size 24-well collagen-coated Transwell culture inserts (Corning) on the luminal side for 3 days at 33°C and then 2 days at 37°C. TY10

cells were exposed to individual IgG from patients with MOG-Ab–associated disorder (acute, n = 15: stable, n = 14), DCs (n = 27), or HCs (n = 9) (500 μg/mL) for 24 hours at 37°C. After the cells were washed, FITC-10-kDa dextran fluorescence (Sigma-Aldrich) was added to the luminal insert (concentration, 1 mg/mL). A total 100 μL of medium was then transferred from the abluminal chamber into 96-well black plates over 40 minutes. Fluorescence signals were calculated at 490/520 nm (absorption/emission) by using a FlexStation 3 Multi-Mode microplate reader (Molecular Devices).

Whole Transcriptome Analyses With RNA-Seq

TY10 cells were exposed to IgGs from 4 patients with MOG-Ab–associated disorder in the acute phase or 3 healthy individuals (500 μg/mL) for 12 hours at 37°C. TY10 cells without incubation with IgGs were used as controls.

The method for the whole transcriptome analysis with RNA-seq was previously described. In brief, total RNA was extracted from TY10 cells using the RNeasy Mini Kit (Qiagen), and messenger RNA was purified as described previously.[20] Complementary DNA libraries were produced using a NEBNext Ultra II RNA Library Prep kit (New England Biolabs) and NEBNextplex Oligos for Illumina, as described previously.[20] In this approach, messenger RNA was fragmented in NEBNext First Strand Synthesis Reaction Buffer at 94°C for 15 minutes in the presence of NEBNext Random Primers and was reverse transcribed with NEBNext Strand Synthesis Enzyme Mix. The library fragments were then concentrated, and index sequences were inserted during polymerase chain reaction amplification. The products were purified using AMPure XP beads (Beckman Coulter), and the quality of the library was confirmed with an Agilent 2200 TapeStation (D1000, Agilent Thermo Fisher). The libraries mixed to equal molecular amounts were sequencing on an Illumina NextSeq DNA sequencer with a 75-bp paired-end cycle sequencing kit (Illumina). The data were then trimmed and mapped to the mouse reference genome GRCm38 release-92 using the CLC Genomics Workbench software program (ver.8.01; Qiagen) as described previously.[20] The mapped read counts were normalized to transcripts per million, which were converted to log2 after the addition of 1. For the volcano plots, p values were calculated with the unpaired Student t test, and the fold change (FC) was determined by subtracting the average values in the HCs from those in patients. Of the genes with a p value of less than 0.05, those for which the FC increased by >50% or decreased by >50% were used for the ingenuity pathway analysis (IPA), which was performed to analyze the detected genes (Qiagen).

Detection of GRP78 Autoantibodies by Western Blotting

The method of Western blotting was previously described.[16] In brief, 2 μg of human full length GRP78 recombinant protein (Abcam) was fractionated and electrophoretically transferred to the polyvinylidene difluoride (PVDF) membranes (Amersham). The GRP78 antibodies (Abcam) and individual IgG (5 μg/mL) from 15 patients with MOG-Ab–associated disorder (acute, n = 15; stable, n = 14), DCs (n = 27), MS (n = 29), HCs (n = 9), and 27 DCs diluted with PBS-T/5% milk were used as the primary antibodies. The PVDF membranes were incubated with each primary antibody for an hour, followed by the anti-human secondary fluorescent antibodies for an hour. For vascular cell adhesion molecule 1 (VCAM-1) and ICAM-1 staining, VCAM-1 antibodies (R&D Systems) and ICAM-1 (Santacruz) were used as the primary antibodies, respectively, followed by an anti-mouse secondary antibody for an hour. The bands were visualized using a chemiluminescence kit (ImmunoStar LD, Japan), and the relative density of each band was calculated with the Quantity One software program (Bio-Rad).

Removal of GRP78 Autoantibodies From MOG-IgG by Immunoprecipitation

The method of GRP78 Ab removal was previously described. In brief, 500 μg/mL of MOG-IgG (patients 1 and 9) was incubated with 5 μg of human embryonic kidney cells 293T cell lysates with or without the overexpression of FLAG-tagged GRP78 (Origene) for 4 hours. After the antigen-antibody immune complexes of GRP78 had precipitated, 40 μL of Red Anti-FLAG M2 Affinity Gel beads (Sigma-Aldrich) was incubated for 2 hours. After centrifuging the sample, the supernatants (MOG-IgG with/without GRP78 antibodies) were used for the analysis.[10] The GRP78 antibodies in both supernatants were detected by a Western blot analysis.

Statistical Analyses

All statistical analyses were performed using the Prism 7 software program (Graph Pad). A paired Student t test (2 sided) was used for single comparison analyses. For multiple comparison analyses, a 1-way analysis of variance was used with the Tukey multiple comparison test when the data were normally distributed or the nonparametric Kruskal-Wallis test when the data were not normally distributed. The Fisher exact probability test was used to calculate the significance of differences in the positivity of GRP78 antibodies among the acute MOG, stable MOG, DC, HC, and MS groups. To assess the association, Pearson correlation coefficients were used. $^{*}p < 0.05$, $^{**}p < 0.01$, and $^{***}p < 0.001$ were considered to have statistical significance.

Data Availability

Data will be shared on reasonable request. Please contact the corresponding author.

Results

IgGs From the Acute Phase of the Patients With MOG-Ab–Associated Disorder Activated BMECs

We first compared the proportion of the nuclear translocation of NF-κB p65 in BMECs among the acute MOG, stable MOG, DC, and HC groups (Figure 1, A–E). The proportion of NF-κB p65 nuclear-positive cells in the acute MOG group

Figure 1 NF-κB p65 Activation and Permeability of Brain Endothelial Cells After Exposure to IgG From Patients With Acute MOG Antibody–Associated Disorder

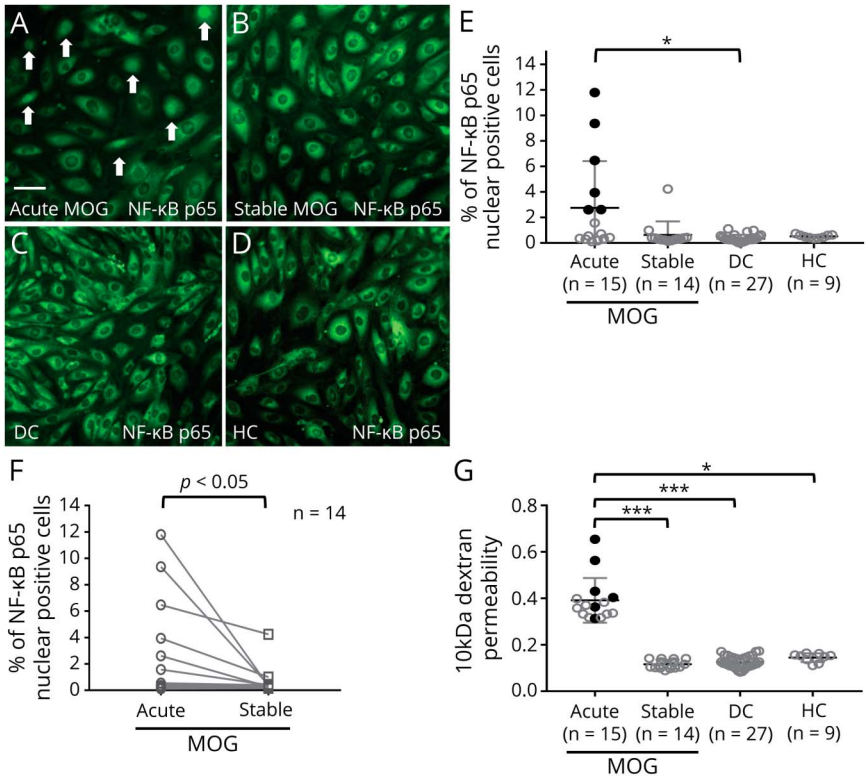

(A–D) Immunostaining of human brain microvascular endothelial cells (TY10 cells) for NF-κB p65 (green) after exposure to IgG (500 μg/mL) from patients with MOG-Ab–associated disorder in the acute phase (acute MOG) (A) or patients with MOG-Ab–associated disorder in the stable phase (stable MOG) (B), DCs (C), or HCs (D). Arrows indicate representative nuclear NF-κB p65–positive cells (A). Images were captured by an In Cell Analyzer 2000. Scale bar, 50 μm. (E) Scatter plots of the number of nuclear NF-κB p65-positive TY10 cells, as determined by high-content imaging after exposure to IgG from patients with MOG-Ab–associated disorder in the acute phase (acute MOG, n = 15), patients with MOG-Ab–associated disorder in the stable phase (stable MOG, n = 14), DCs (n = 27), and HCs (n = 7). The data were normalized to cultures that had not been exposed to human IgG and are shown as the mean ± standard error of the mean from 4 independent experiments, performed in technical triplicate. Black dots show the 6 samples inducing the 6 highest degrees of nuclear translocation of NF-κB. The *p* values were determined by the nonparametric Kruskal-Wallis test (*$p < 0.05$). (F) The proportion of nuclear NF-κB p65 nuclear-positive cells between the acute and stable phase in the same individual is shown. The *p* values were determined by a paired 2-tailed *t* test (G) Scatter plots of the 10-kDa dextran permeability of TY10 cells after exposure to acute MOG-IgG (n = 15), stable MOG-IgG (n = 14), DC-IgG (n = 27), or HC-IgG (n = 7). Black dots show the 6 samples inducing the 6 highest degrees of nuclear translocation of NF-κB. The *p* values were determined by the nonparametric Kruskal-Wallis test (*$p < 0.05$, ***$p < 0.001$ vs the stable MOG, DC, and HC groups). DC = disease control; HC = healthy control; MOG = myelin oligodendrocyte glycoprotein; MOG-Ab = myelin oligodendrocyte glycoprotein antibody.

was significantly greater than in the DC group (Figure 1E). The proportion of NF-κB p65 nuclear-positive cells was significantly decreased between the acute and stable MOG in the same individual (Figure 1F). The permeability was found to be significantly increased after incubation with IgG from the acute MOG group compared with that from the stable MOG, DC, or HC groups (Figure 1G). In a time course study (6, 12, 18, and 24 hours), the 10-kDa dextran permeability in BMECs was increased after >12 hours of incubation with 2 IgGs from MOG patients (patients 1 and 9) (eFigure 1, links.lww.com/NXI/A602). Furthermore, a Western blot analysis showed that the VCAM-1 expression was significantly increased after exposure to IgG from the acute MOG group compared with that from the stable MOG, DC, and HC groups (Figure 2, A and B). The ICAM-1 expression was significantly upregulated after incubation with IgG from the acute MOG group compared with that from the stable MOG and HC groups (Figure 2, A and D). High-content imaging revealed that the ICAM-1 expression was significantly increased after exposure to IgG from the acute MOG/DC group compared with that from the HC group (Figure 2, D and E).

Profiling of Altered Gene Expression in BBB Endothelial Cells After IgG Exposure From the Acute Phase of the Patients With MOG-Ab–Associated Disorder

We selected IgG from 4 patients with MOG-Ab–associated disorder presenting with myelitis or cortical encephalitis and showing an elevated effect on the induction of NF-κB p65 nuclear translocation of TY10 (patients 1, 3, 5, and 9 in Table) for RNA-seq. A whole transcriptome analysis using RNA-seq in BMECs after exposure to IgG from the patients with MOG-Ab–associated disorder (n = 4) and HCs (n = 3) was performed to identify important signaling pathway. BMECs without exposure to IgGs were used as controls. In TY10 cells, over 32,000 genes were detected from approximately 30 million reads in each sample. Volcano plots (Figure 2A) and heat maps (eFigure 2, links.lww.com/NXI/A603) at the same

Figure 2 Changes in the VCAM-1 and ICAM-1 Expression After IgG Exposure From Acute MOG Antibody–Associated Disorders

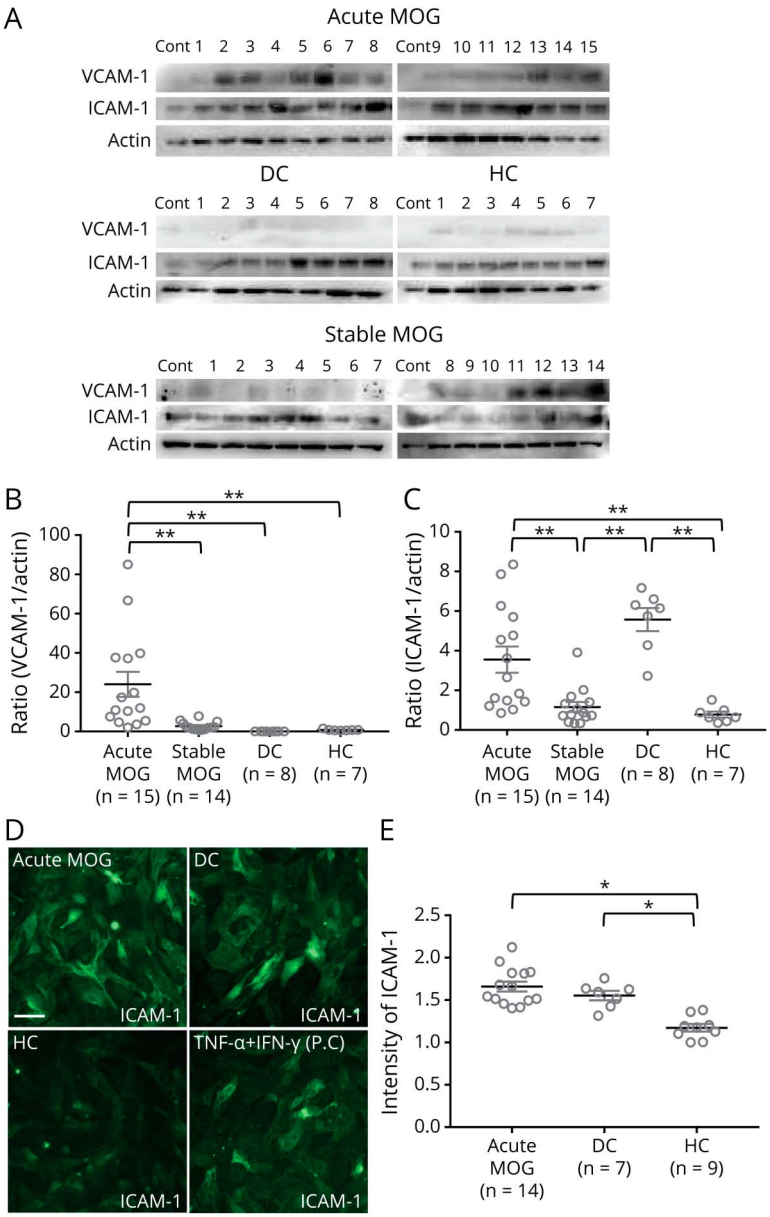

(A) Western blotting of VCAM-1 or ICAM-1 in TY10 after exposure to IgG (500 μg/mL) from patients with MOG-Ab–associated disorder in the acute phase (acute MOG, n = 15), the stable phase (stable MOG, n = 14), DCs (n = 8), or HCs (n = 7). (B) (C) Scatter plots of quantification by Western blotting for VCAM-1 (B) or ICAM-1 (C) in relation to actin. Each scatter plot reflects the combined densitometry data (mean ± standard error of the mean). The *p* values were determined by a 1-way analysis of variance followed by the Tukey multiple comparison test (**$p < 0.01$ vs the DC or HC group followed by the Tukey multiple comparison test). (D) Immunostaining of human brain microvascular endothelial cells (TY10 cells) for ICAM-1 (green) after exposure to IgG (500 μg/mL) from patients with MOG-Ab–associated disorder in the acute phase (acute MOG), DCs, or HCs. Tumor necrosis factor-α and interferon-γ stimulation served as a positive control. Image of ICAM-1 captured by an In Cell Analyzer 2000. Scale bar, 50 μm. (E) Scatter plots of intensity of ICAM-1, as determined by high-content imaging after exposure to IgG from patients with MOG-Ab–associated disorder in the acute phase (acute MOG, n = 14), DCs (n = 7), and HCs (n = 9). The data were normalized to cultures that had not been exposed to human IgG and are shown from 3 independent experiments. The *p* values were determined by a 1-way ANOVA followed by the Tukey multiple comparison test (*$p < 0.05$ vs the DC or HC group followed by the Tukey multiple comparison test). ANOVA = analysis of variance; DC = disease control; HC = healthy control; ICAM-1 = intercellular adhesion molecule 1; MOG = myelin oligodendrocyte glycoprotein; MOG-Ab = myelin oligodendrocyte glycoprotein antibody; VCAM-1 = vascular cell adhesion molecule 1.

p values and FC revealed that 189 genes were significantly differentially expressed (FC > 1.5; $p < 0.05$), including 83 upregulated genes and 106 downregulated genes, between the patients with MOG-Ab–associated disorder (n = 4) and HC/control groups (n = 4) (eFigure 1, links.lww.com/NXI/A602). Next, Ingenuity Pathway Analysis (an IPA) was performed using the above upregulated or downregulated genes to determine the signaling pathway of BMECs after exposure to IgGs from the acute phase of patients with MOG-Ab–associated disorder. In the network analysis of the upregulated genes, *NF-κB* was detected in the center of the network analysis, and *PLAAT4* and *TNFRSF6B* were observed as upstream molecules of NF-κB (Figure 3B). In the network analysis of downregulated genes, *NQO1* and *DNAJB1* were detected in the center of the network analysis, suggesting that oxidative stress had been induced (Figure 3C).

IgGs From the Acute Phase of the Patients With MOG-Ab–Associated Disorder Reduced Protective Proteins Against Oxidative Stress in BBB Endothelial Cells

To confirm the data suggested by RNA-seq, the change in amounts of protective proteins against oxidative stress after exposure to IgGs from the patients with MOG-Ab–associated disorder was observed. We selected 14 IgGs from the acute MOG group, 7 IgGs from the DC group (all samples from patients with amyotrophic lateral sclerosis), and 9 IgGs from the HC group for this purpose. High-content imaging system

Figure 3 Whole Transcriptome Analysis With RNA-Seq of TY10 After Exposure to IgG From Patients With MOG Antibody–Associated Disorders

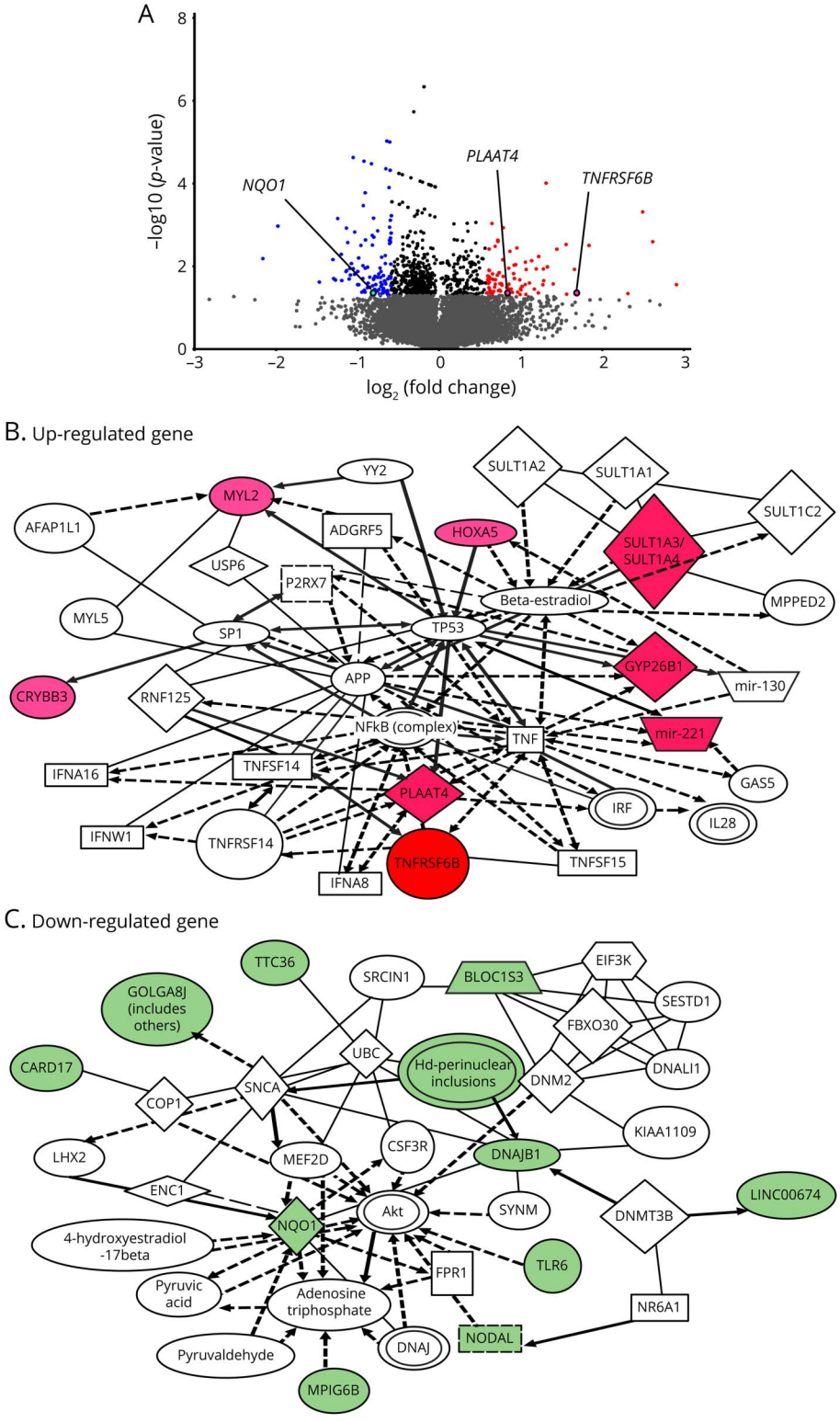

TY10 cells were incubated with IgG from the patients with MOG-Ab–associated disorder (n = 4) and healthy controls (n = 3). TY10 cells without exposure to IgGs were also used as control. Over 32,000 genes were detected from approximately 30 million reads in each sample. (A) Volcano plots (FC > 1.5; $p < 0.05$) revealed that 189 genes were significantly differentially expressed (FC > 1.5; $p < 0.05$), including 83 upregulated genes (red) and 106 downregulated genes (blue), between the patients with MOG-Ab–associated disorder (n = 4) and healthy control (n = 3)/control (n = 1) groups (total n = 4). (B) In the network analysis of upregulated genes, NF-κB was detected in the center of the network analysis. The red nodes show the upregulated genes in the RNA-seq analysis (FC > 1.5; $p < 0.05$). (C) In the network analysis of downregulated genes, NQO1 and DNAJB1 were detected in the center of the network analysis. The green nodes show the downregulated genes in the RNA-seq analysis (FC < 1.5; $p < 0.05$). DC = disease control; HC = healthy control; FC = fold change; ICAM-1 = intercellular adhesion molecule 1; MOG = myelin oligodendrocyte glycoprotein; MOG-Ab = myelin oligodendrocyte glycoprotein antibody; VCAM-1 = vascular cell adhesion molecule 1.

revealed that the expression of NQO1 and Nrf2 protein in BMECs and the mitochondria membrane potential (red/green ratio using JC-1 dye) were significantly decreased after exposure to IgGs from the acute phase of the patients with MOG-Ab–associated disorder compared with that from DCs or HCs (Figure 4, A–E). Furthermore, a Western blot analysis showed that the amount of Nrf2 protein of TY10 cells was also decreased after exposure to IgGs from the acute phase of

Figure 4 Changes in the Protective Proteins Against Oxidative Stress After IgG Exposure From Acute MOG Antibody–Associated Disorders

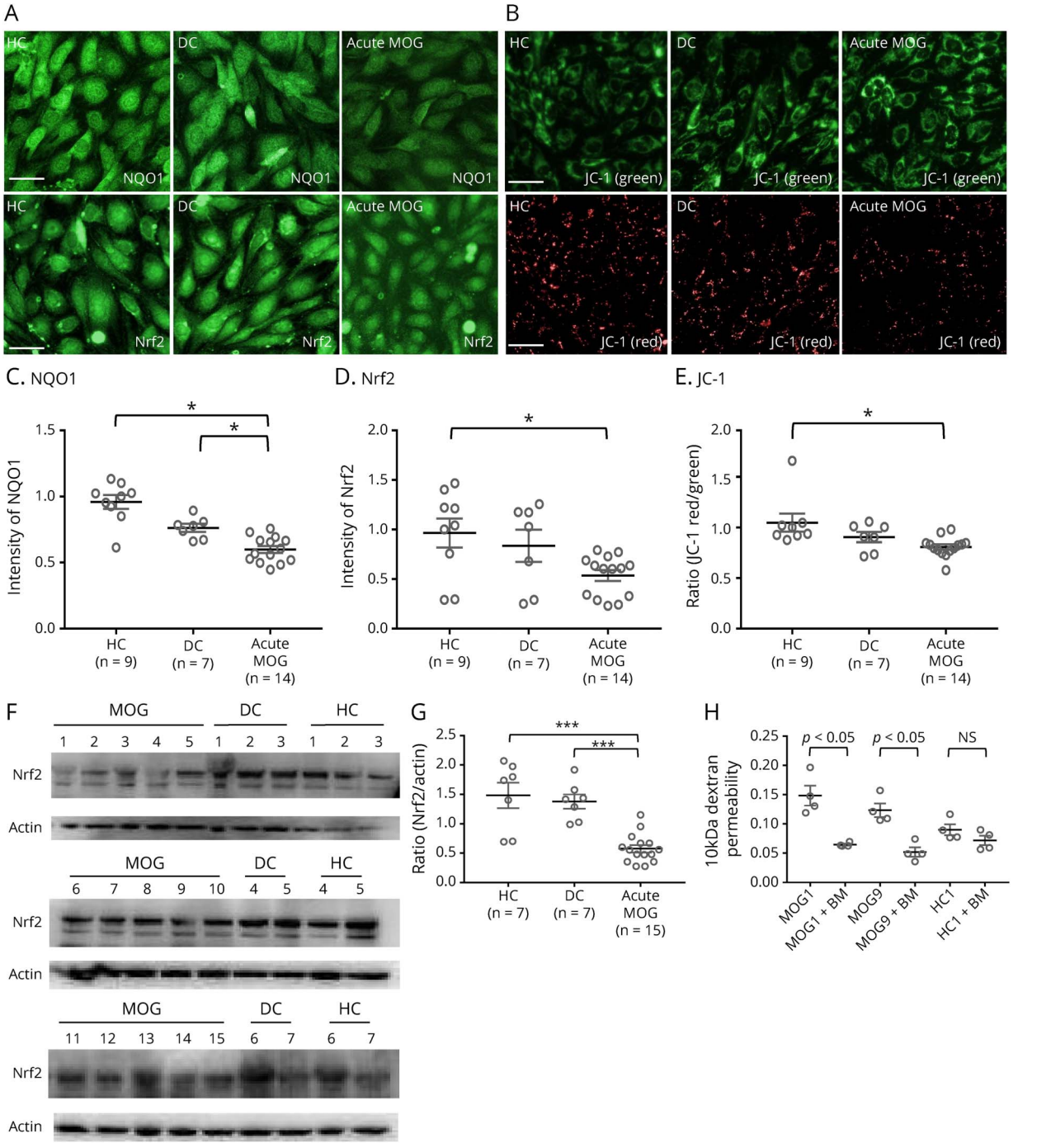

(A, B) Immunostaining of human brain microvascular endothelial cells (TY10 cells) for NQO1 or Nrf2 (green), or JC-1 (green/red) after exposure to IgG (500 μg/mL) from patients with MOG-Ab–associated disorder in the acute phase (acute MOG), DCs, or HCs (upper, NQO1/lower, Nrf2). Images were captured by an In Cell Analyzer 2000. The JC-1 red/green intensity ratio reflects the mitochondria potential. Scale bar, 50 μm. (C–E) Scatter plots of the intensity of NQO1 or Nrf2, or JC-1 red/green intensity ratio in TY10 cells, as determined by high-content imaging after exposure to IgG from patients with MOG-Ab–associated disorder in the acute phase (acute MOG, n = 14), DCs (n = 9), and HCs (n = 7). The data were normalized to cultures that had not been exposed to human IgG and are shown from 3 independent experiments. The *p* values were determined by a 1-way ANOVA followed by the Tukey multiple comparison test (*$p < 0.05$ vs the DC or HC group followed by the Tukey multiple comparison test). (F) Western blotting of Nrf2 in TY10 after exposure to acute MOG-IgG (n = 15), DC-IgG (n = 7), or HC-IgG (n = 7) (500 μg/mL). (G) Scatter plots of quantification by Western blotting for Nrf2 in relation to actin. Each scatter plot reflects the combined densitometry data (mean ± standard error of the mean). The *p* values were determined by a 1-way ANOVA followed by the Tukey multiple comparison test (***$p < 0.001$ vs the DC or HC group followed by the Tukey multiple comparison test). (H) Effect of 2 MOG-IgG (Pts 1 and 9, 250 μg/mL) on 10-kDa dextran permeability on BMECs after incubation with and without bardoxolone methyl (MOG vs MOG + bardoxolone methyl), which has the effect of activating Nrf2 and inhibiting NF-κB activation. ANOVA = analysis of variance; BMEC = brain microvascular endothelial cell; DC = disease control; HC = healthy control; MOG = myelin oligodendrocyte glycoprotein; MOG-Ab = myelin oligodendrocyte glycoprotein antibody.

Figure 5 Western Blotting of GRP78 Autoantibodies in IgG From Patients With MOG Antibody–Associated Disorders

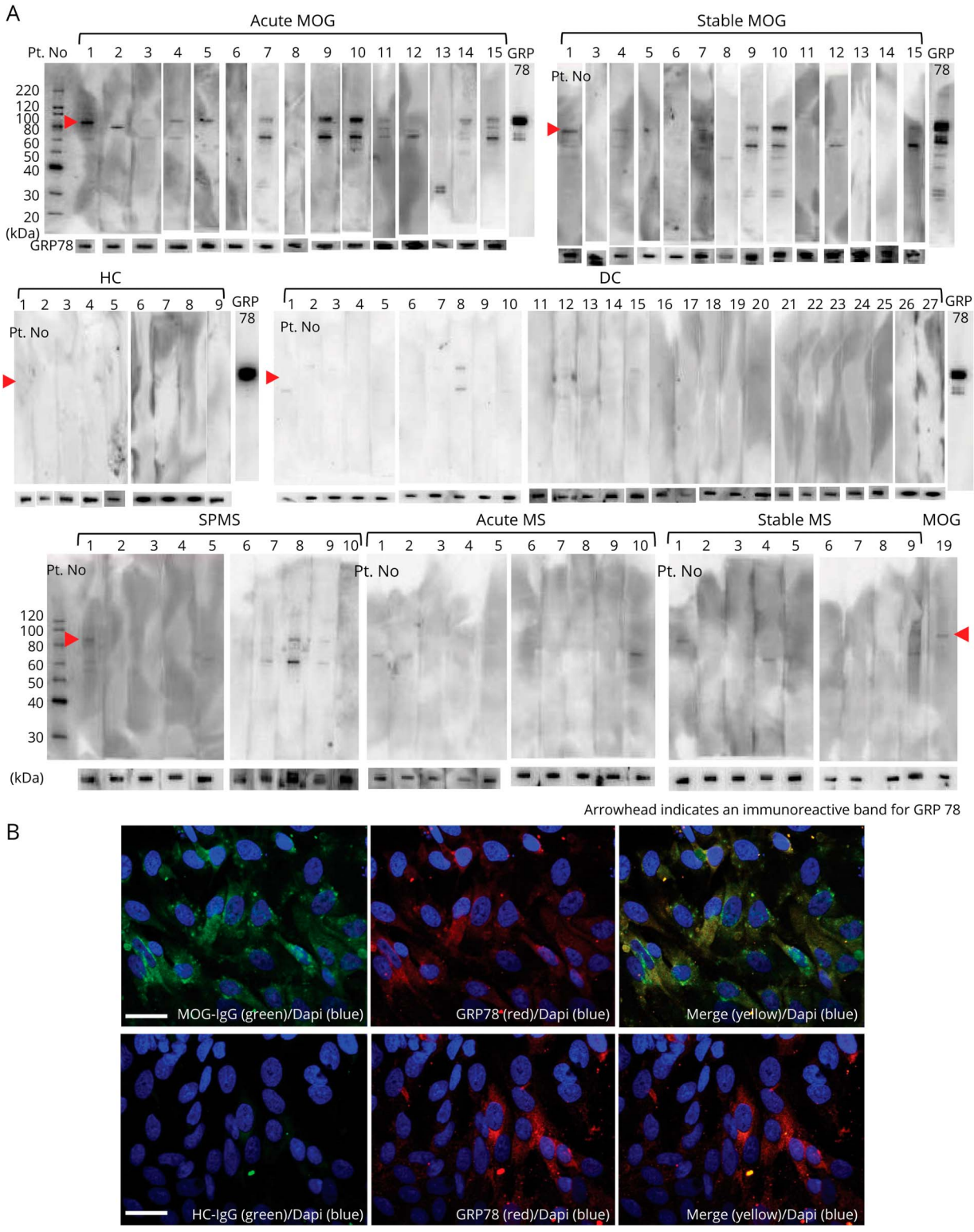

(A) The results of Western blotting of individual IgG samples (5 μg/mL) from patients with acute and stable MOG, MS, DCs, and HCs, as determined using recombinant human GRP78 protein prepared from *Escherichia coli*. The arrowhead indicates an immunoreactive band corresponding to GRP78. Rabbit anti-GRP78 antibodies were used as the positive control. The rate of GRP78 antibody positivity: (1) the acute MOG group (10/15, 67% [95% CI 38%–88%]), (2) stable MOG group (5/14, 36% [95% CI 13%–65%]), (3) MS group (total MS: 4/29, 14% [95% CI 4%–32%]), (4) DC group (3 of 27, 11% [95% CI 2%–29%]), (5) HC group (0 of 9, 0% [95% CI 0%]), (6) secondary progressive MS group (3 of 10, 30% [95% CI 6%–65%]), (7) acute MS group (0 of 10, 0% [95% CI 0%], and (8) stable MS group (1 of 9, 11% [95% CI 0.3%–48%]). (B) Immunofluorescence labeling of TY10 cells with MOG-IgG (50 μg/mL) (green) and commercial anti-GRP78 antibodies (red) shows colocalization of the 2 proteins (merged in yellow). Scale bar, 50 μm. CI = confidence interval; DC = disease control; HC = healthy control; MOG = myelin oligodendrocyte glycoprotein.

Figure 6 Effect of the Removal of GRP78 Autoantibodies From Acute MOG-IgG on the NF-κB p65 Nuclear Translocation in BMECs

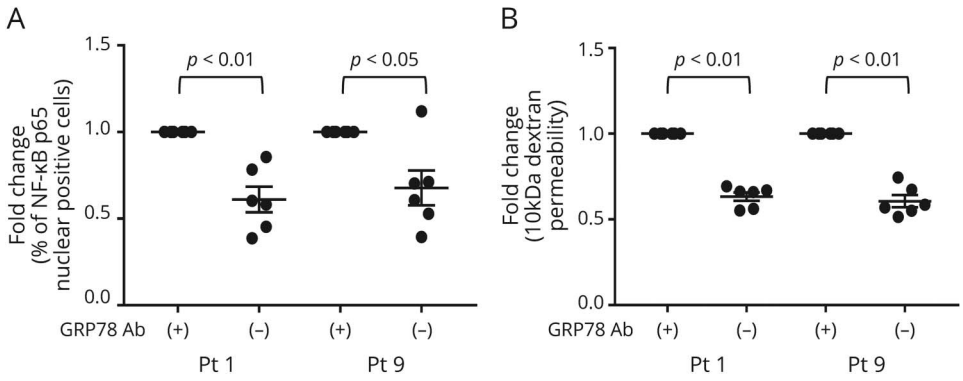

The removal of GRP78 antibodies from 2 acute MOG-IgGs (500 μg/mL, patients 1 and 9) with MOG-Ab–associated disorder significantly decreased the NF-κB nuclear translocation of BMECs (A) and the 10-kDa dextran permeability (B). Data are shown as the mean ± standard error of the mean of 6 independent experiments. Statistical significance was determined by a paired 2-tailed *t* test. GRP78 Ab (+), MOG-IgG with GRP78 autoantibodies; GRP78 Ab (−), MOG-IgG without GRP78 autoantibodies. BMEC = brain microvascular endothelial cell; MOG = myelin oligodendrocyte glycoprotein; MOG-Ab = myelin oligodendrocyte glycoprotein antibody.

patients with MOG-Ab–associated disorder compared with that from DCs or HCs (Figure 4, F and G). The effect of MOG-IgG (MOG1 and 9) on 10-kDa dextran permeability in BMECs was reversed after incubation with bardoxolone methyl, which has the effect of activating Nrf2 and inhibiting NF-κB activation.

Detection of GRP78 Autoantibodies in MOG-Ab–Associated Disorder

The GRP78 autoantibodies were detected in the IgG from patients with MOG-Ab–associated disorder by Western blotting. The rate of GRP78 antibody positivity observed in the acute MOG group (10/15, 67% [95% confidence interval {CI} 38%–88%]) was significantly higher than that in the stable MOG group (5/14, 36% [95% CI 13%–65%]), the MS group (total MS: 4/29, 14% [95% CI 4%–32%]), the DC group (3 of 27, 11% [95% CI 2%–29%]), or the HC group (0 of 9, 0% [95% CI 0%]) (Figure 5A). The rate of this antibody positivity in the acute MOG group (10/15, 67% [95% CI 38%–88%]) was also significantly higher than that in secondary progressive MS (3/10, 30% [95% CI 6%–65%]), acute MS (0/10, 0% [95% CI 0%] and stable MS (1/9, 11% [95% CI 0.3%–48%]. Double immunostaining with commercial anti-GRP78 Abs and IgG from GRP78 antibody–positive patients with MOG-Ab–associated disorder demonstrated colocalization in BMECs (Figure 5B).

Removal of GRP78 Antibodies in MOG-Ab–Associated Disorder

We selected GRP78 antibody–positive IgGs from 2 acute MOG patients who showed a ΔEDSS score of >5 and the highest effect on the induction of NF-κB p65 nuclear translocation of TY10 (patients 1 and 9 in Table). We prepared 2 MOG-IgGs (1 with and 1 without GRP78 antibodies) from these MOG patients using immunoprecipitation. Complete depletion of GRP78 antibodies was observed by a Western blot analysis (eFigure 3, links.lww.com/NXI/A663). The removal of GRP78 antibodies from MOG-IgGs from these 2 patients with MOG-Ab–associated disorder resulted in a significant reduction in NF-κB nuclear translocation and decreased permeability of BMECs (Figure 6, A and B).

There was no significant association between the clinical phenotype/ΔEDSS score and positivity for GRP78 antibodies/number of NF-κB p65 nuclear-positive BMECs after MOG-IgG exposure (data not shown).

Discussion

MOG is specifically expressed in oligodendrocytes, not in BMECs, so MOG-Abs itself cannot bind and react to the BBB via immune activation.[21] In the present study, we demonstrated that IgG derived from MOG-Ab–associated disorder activated BBB endothelial cells; fraction of TY10 with the NF-κB p65 nuclear translocation was significantly increased after the acute MOG group than that after the DC group and significantly lower in the same individual MOG patients between the acute and stable phases. The permeability of the monolayer TY10 cells was significantly higher in the acute MOG group than in the stable MOG/DC/HC group. The amount of VCAM-1 and ICAM-1 protein in the TY10 cells was also higher in the acute MOG group than that in the stable MOG and HC group. These results suggest that IgG from the acute-phase MOG patients induced endothelial activation and increased the BBB permeability. Whole RNA-seq and the pathway analysis revealed that the genes associated with NF-κB signal and oxidative stress were significantly changed after exposure to IgG from GRP78 antibody–positive patients with MOG-Ab–associated disorder compared with HCs. In addition, the amount of NQO1 and Nrf2 protein and the mitochondrial membrane potential were lower in the acute MOG group than in the DC and/or HC groups, and activation of Nrf2 reversed the increased permeability of TY10 cells after MOG-IgG exposure, suggesting that IgG from acute-phase MOG patients induced oxidative stress in TY10 cells. Furthermore, the positive rate of GRP78 autoantibodies in the acute MOG

group was significantly higher than that in the stable MOG, DC, MS, and HC groups (acute MOG 66% vs stable MS 36%, MS 14%, DCs 11%, and HCs 0%). Double immunostaining with commercial anti-GRP78 antibody and MOG-IgG demonstrated colocalization in TY cells, suggesting that MOG-IgG reacted with GRP78. Depletion of GRP78 antibodies from acute MOG-IgG reduced the effect on NF-κB p65 nuclear translocation and BMEC permeability. These results suggest that IgGs from patients with MOG-Ab–associated disorder induced the disruption of the BBB via the NF-κB signaling and the oxidative stress, and GRP78 antibodies were associated with BBB breakdown in patients with MOG-Ab–associated disorder. Unfortunately, we were unable to perform the in vivo experiments in which GRP78-IgG–seropositive and –seronegative myelin oligodendrocyte glycoprotein antibodies-associated disorder sera were administered peripherally to MOG-EAE animals to evaluate the relationship between GRP78 autoantibodies and BBB permeability in the present study.

We recently reported that GRP78 autoantibodies were a potential biomarker associated with the BBB breakdown in NMO.[15] In addition, the positivity rate of GRP78 autoantibodies in the longitudinally extensive transverse myelitis phenotype of NMOSD was higher than that in the optic neuritis (ON) phenotype (longitudinally extensive transverse myelitis 71% vs ON 17%), and positivity of GRP78 antibodies was associated with an increased clinical severity (ΔEDSS score) in patients with NMOSD and BBB permeability in our in vitro BBB model.[16] The present study showed that GRP78 antibodies were associated with MOG-Ab–associated disorder beyond NMOSD, suggesting that these antibodies may be able to be triggered in the activation of BMECs in the disease as well as NMOSD.

NQO1 is a cytosolic homodimeric flavoprotein that catalyzes the 2-electron reduction of quinones, and its production is induced under many stress conditions, including oxidative stress, to protect against cellular damage. Nrf2 plays an important role in the regulation of many antioxidant enzyme genes, such as NQO1.[22] A reduction in the Nrf2 signal leads to the induction of oxidative stress via a decrease in NQO1 and increase in inflammatory signaling pathways, including that of NF-κB, resulting in dysfunction of the BBB endothelial cells and increased paracellular permeability.[23] Bardoxolone methyl activates the Nrf2 system and protects the cells against oxidative stress through the inhibition of reactive oxygen species generation.[24] BMEC permeability induced by MOG-IgG was decreased after incubation with bardoxolone methyl in the present study. We revealed the role of GRP78 antibody in MOG-Ab–associated disorder on the BBB dysfunction: the induction of inflammation via NF-κB and the increase in oxidative stress through Nrf2 on BBB endothelial cells.

We next evaluated clinical data using statistical analyses to address whether NF-κB nuclear translocation/permeability of BMECs and GRP78 antibodies was correlated with the clinical data in MOG-Ab–associated disorder. However, we failed to observe any significant association between NF-κB nuclear translocation/permeability/GRP78 antibodies and the clinical phenotype/disease activity/clinical data. Multiple potential factors, including the small sample size, low assay sensitivity by Western blotting, a lack of detection of GRP78 antibodies titer, a lack of information of pathogenic autoantibody epitopes, and a relatively poor understanding of clinical metric and the disease pathophysiology, may have contributed to the lack of a correlation. The establishment of a better assay for GRP78 autoantibodies, including an ELISA using pathogenic antibody epitopes and a CBA to determine the GRP78 antibody titer, will be needed to address these important questions.

A case report described 2 patients with MOG-Ab–associated encephalitis mimicking small-vessel CNS vasculitis: Brain biopsy samples of abnormal MRI scans from these 2 patients revealed prominent lymphocytic infiltration of the wall of the small vessels, including T and B lymphocytes with edema, perivascular demyelination, and reactive gliosis, without fibrinoid necrosis.[25] The present study showed the upregulation of VCAM-1 in BBB endothelial cells after exposure to IgG from patients with MOG-Ab–associated disorder. The overexpression of VCAM-1 in the brain microvasculature may induce lymphocytic infiltration around the small vessels of the CNS.[26] GRP78 antibodies may play a role in inducing the inflammation of small vessels of the brain in MOG-Ab–associated encephalitis via the upregulation of the VCAM-1 and ICAM-1 expression.

In conclusion, our data show that GRP78 autoantibodies play a role in increasing the permeability of BMECs, thus suggesting the potential ability to the entry of pathogenic MOG-Abs into the CNS in MOG-Ab–associated disorder. Further studies using better assay, including an ELISA and CBA, to determine the GRP78 antibody titer will be required to understand the association between the clinical phenotype of the disease and GRP78 antibodies. An in vivo study will be needed to confirm the association between GRP78 autoantibodies and BBB permeability.

Study Funding

Funding organizations had no role in the design or conduct of this research. This research was supported by research grants (Nos. 18K07526 and 20H00529) from the Japan Society for the Promotion of Science, Tokyo, Japan, Takeda research foundation, and a research grant from Health and Labour Sciences Research Grants for research on intractable diseases (Neuroimmunological Disease Research Committee) from the Ministry of Health, Labour and Welfare of Japan.

Disclosure

The authors report no financial disclosure relevant to the submitted manuscripts. T. Kanda received speaking fees

outside this work from Teijin Pharma Limited, Nihon Pharmaceutical Co., Ltd., Kaketsuken, Mitsubishi Tanabe Pharma, Takeda Pharmaceutical company, Novartis, and Biogen. Go to Neurology.org/NN for full disclosures.

Publication History

Received by *Neurology: Neuroimmunology & Neuroinflammation* January 11, 2021. Accepted in final form May 25, 2021.

Appendix Authors

Name	Location	Contribution
Fumitaka Shimizu, MD, PhD	Department of Neurology and Clinical Neuroscience, Yamaguchi University Graduate School of Medicine, Ube, Japan	Drafting/revision of the manuscript for content, including medical writing for content; major role in the acquisition of data; study concept or design; and analysis or interpretation of data
Ryo Ogawa, MD, PhD	Department of Neurology, Tohoku University Graduate School of Medicine, Sendai, Japan	Analysis or interpretation of data
Yoichi Mizukami, MD, PhD	Center for Gene Research, Yamaguchi University, Ube, Japan	Analysis or interpretation of data
Kenji Watanabe, PhD	Center for Gene Research, Yamaguchi University, Ube, Japan	Analysis or interpretation of data
Kanako Hara	Department of Neurology and Clinical Neuroscience, Yamaguchi University Graduate School of Medicine, Ube, Japan	Major role in the acquisition of data
Chihiro Kadono	Department of Neurology and Clinical Neuroscience, Yamaguchi University Graduate School of Medicine, Ube, Japan	Major role in the acquisition of data
Toshiyuki Takahashi, MD, PhD	Department of Neurology, Tohoku University Graduate School of Medicine, Sendai, Japan; Department of Neurology, National Hospital Organization Yonezawa Hospital, Yonezawa, Japan	Analysis or interpretation of data
Tatsuro Misu, MD, PhD	Department of Neurology, Tohoku University Graduate School of Medicine, Sendai, Japan	Analysis or interpretation of data
Yukio Takeshita, MD, PhD	Department of Neurology and Clinical Neuroscience, Yamaguchi University Graduate School of Medicine, Ube, Japan	Analysis or interpretation of data
Yasuteru Sano, MD, PhD	Department of Neurology and Clinical Neuroscience, Yamaguchi University Graduate School of Medicine, Ube, Japan	Analysis or interpretation of data
Miwako Fujisawa, MD	Department of Neurology and Clinical Neuroscience, Yamaguchi University Graduate School of Medicine, Ube, Japan	Major role in the acquisition of data
Toshihiko Maeda, MD, PhD	Department of Neurology and Clinical Neuroscience, Yamaguchi University Graduate School of Medicine, Ube, Japan	Major role in the acquisition of data
Ichiro Nakashima, MD, PhD	Department of Neurology, Tohoku Medical and Pharmaceutical University, Sendai, Japan	Drafting/revision of the manuscript for content, including medical writing for content, and analysis or interpretation of data
Kazuo Fujihara, MD, PhD	Department of Multiple Sclerosis Therapeutics, Fukushima Medical University, Fukushima, Japan	Drafting/revision of the manuscript for content, including medical writing for content, and analysis or interpretation of data
Takashi Kanda, MD, PhD	Department of Neurology and Clinical Neuroscience, Yamaguchi University Graduate School of Medicine, Ube, Japan	Drafting/revision of the manuscript for content, including medical writing for content, and study concept or design

References

1. Fujihara K. Neuromyelitis optica spectrum disorders: still evolving and broadening. *Curr Opin Neurol*. 2019;32(3):385-394.
2. Cobo-Calvo A, Vukusic S, Marignier R. Clinical spectrum of central nervous system myelin oligodendrocyte glycoprotein autoimmunity in adults. *Curr Opin Neurol*. 2019;32(3):459-466.
3. Dos Passos GR, Oliveira LM, da Costa BK, et al. MOG-IgG-Associated optic neuritis, encephalitis, and myelitis: lessons learned from neuromyelitis optica spectrum disorder. *Front Neurol*. 2018;9(4):217.
4. Reindl M, Jarius S, Rostasy K, Berger T. Myelin oligodendrocyte glycoprotein antibodies: how clinically useful are they? *Curr Opin Neurol*. 2017;30(3):295-301.
5. Spadaro M, Gerdes LA, Mayer MC, et al. Histopathology and clinical course of MOG-antibody-associated encephalomyelitis. *Ann Clin Transl Neurol*. 2015;2(3):295-301.
6. Wang JJ, Jaunmuktane Z, Mummery C, Brandner S, Leary S, Trip SA. Inflammatory demyelination without astrocyte loss in MOG antibody-positive NMOSD. *Neurology*. 2016;87(2):229-231.
7. Zhou L, Huang Y, Li H, et al. MOG-antibody associated demyelinating disease of the CNS: a clinical and pathological study in Chinese Han patients. *J Neuroimmunol*. 2017;305(15):19-28.
8. Körtvélyessy P, Breu M, Pawlitzki M, et al. ADEM-like presentation, anti-MOG antibodies, and MS pathology: two case reports. *Neurol Neuroimmunol Neuroinflamm*. 2017;4(3):e335.
9. Jarius S, Metz I, König FB, et al. Screening for MOG-IgG and 27 other anti-glial and anti-neuronal autoantibodies in 'pattern II multiple sclerosis' and brain biopsy findings in a MOG-IgG-positive case. *Mult Scler*. 2016;22(12):1541-1549.
10. Spadaro M, Winklmeier S, Beltrán E, et al. Pathogenicity of human antibodies against myelin oligodendrocyte glycoprotein. *Ann Neurol*. 2018;84(2):315-328.
11. Shimizu F, Sano Y, Takahashi T, et al. Sera from neuromyelitis optica patients disrupt the blood-brain barrier. *J Neurol Neurosurg Psychiatry*. 2012;83(3):288-297.
12. Tasaki A, Shimizu F, Sano Y, et al. Autocrine MMP-2/9 secretion increases the BBB permeability in neuromyelitis optica. *J Neurol Neurosurg Psychiatry*. 2014;85(4):419-430.
13. Shimizu F, Nishihara H, Sano Y, et al. Markedly increased IP-10 production by blood-brain barrier in neuromyelitis optica. *Plos One*. 2015;10(3):e0122000.
14. Shimizu F, Tasaki A, Sano Y, et al. Sera from remitting and secondary progressive multiple sclerosis patients disrupt the blood-brain barrier. *Plos One*. 2014;9(3):e92872.
15. Shimizu F, Schaller KL, Owens GP, et al. Glucose-regulated protein 78 autoantibody associates with blood-brain barrier disruption in neuromyelitis optica. *Sci Transl Med*. 2017;9(397):eaai9111.
16. Shimizu F, Takeshita Y, Hamamoto Y, et al. GRP 78 antibodies are associated with clinical phenotype in neuromyelitis optica. *Ann Clin Transl Neurol*. 2019;6(10):2079-2087.
17. Ramanathan S, Mohammad S, Tantsis E, et al. Clinical course, therapeutic responses and outcomes in relapsing MOG antibody-associated demyelination. *J Neurol Neurosurg Psychiatry*. 2018;89(2):127-137.
18. Spadaro M, Gerdes LA, Krumbholz M, et al. Autoantibodies to MOG in a distinct subgroup of adult multiple sclerosis. *Neurol Neuroimmunol Neuroinflamm*. 2016;3(5):e257.

19. Sano Y, Shimizu F, Abe M, et al. Establishment of a new conditionally immortalized human brain microvascular endothelial cell line retaining an in vivo blood-brain barrier function. *J Cell Physiol*. 2010;225(2):519-528.
20. Kohno M, Kobayashi S, Yamamoto T, et al. Enhancing calmodulin binding to cardiac ryanodine receptor completely inhibits pressure-overload induced hypertrophic signaling. *Commun Biol*. 2020;3(1):714.
21. oJhns TG, Bernard CC. The structure and function of myelin oligodendrocyte glycoprotein. *J Neurochem*. 1999;72(1):1-9.
22. Nguyen T, Nioi P, Pickett CB. The Nrf2-antioxidant response element signaling pathway and its activation by oxidative stress. *J Biol Chem*. 2009;284(20):13291-13295.
23. Li W, Suwanwela NC, Patumraj S. Curcumin by down-regulating NF-kB and elevating Nrf2, reduces brain edema and neurological dysfunction after cerebral I/R. *Microvasc Res*. 2016;106:117-127.
24. Kanda H, Yamawaki K. Bardoxolone methyl: drug development for diabetic kidney disease. *Clin Exp Nephrol*. 2020;24(10):857-864.
25. Patterson K, Iglesias E, Nasrallah M, et al. Anti-MOG encephalitis mimicking small vessel CNS vasculitis. *Neurol Neuroimmunol Neuroinflamm*. 2019;6(2):e538.
26. Ferrario F, Vanzati A, Pagni F. Pathology of ANCA-associated vasculitis. *Clin Exp Nephrol*. 2013;17(5):652-658.